(10) B. Volasek, *Croat. Chem. Acta*, **33**, 181 (1961).
(11) J. R. Geichman, P. R. Ogle, and L. R. Swaney, Goodyear Atomic Corporation Report GAT-T-809 (1961).
(12) I. Sheft, H. H. Hyman, R. Adams, and J. J. Katz, *J. Am. Chem. Soc.*, **83**, 291 (1961).
(13) U.S. Patent 3 039 846 (1962).
(14) J. R. Geichman, E. A. Smith, and P. R. Ogle, *Inorg. Chem.*, **2**, 1012 (1963).
(15) S. Katz, Oak Ridge National Laboratory Report ORNL 3497 (1964).
(16) S. Katz, *Inorg. Chem.*, **3**, 1958 (1964).
(17) L. McNeese, Oak Ridge National Laboratory Report ORNL 3494 (1964).
(18) J. G. Malm, H. Selig, and S. Siegel, *Inorg. Chem.*, **5**, 130 (1966).
(19) S. Katz, *Inorg. Chem.*, **5**, 666 (1966).
(20) I. Peka, *Collect. Czech. Chem. Commun.*, **37**, 4245 (1966).
(21) I. Peka, *Collect. Czech. Chem. Commun.*, **31**, 4469 (1966).
(22) I. Peka, *Collect. Czech. Chem. Commun.*, **32**, 426 (1967).
(23) A. T. Sadikova and N. S. Nikolaev, *Atomnaia Energuia*, **25**, 422 (1968).
(24) A. T. Sadikova, G. G. Sadikov, and N. S. Nikolaev, *Atomnaia Energuia*, **26 (3)**, 239 (1969).
(25) G. Besnard, A. J. Dianoux, O. Hartmanshenn, H. Marquet-Ellis, and N. H. Nghi, *Commis. Energ. At.* [*Fr.*], *Rapp.*, R-3732 (1969).
(26) A. Paillet, Thesis, Lyon, France, 1972.
(27) R. Bougon, R. M. Costes, J. P. Desmoulin, J. Michel, and J. L. Person, *Inorg. Nucl. Chem. Suppl.*, 99 (1976).
(28) P. Charpin, J. Michel, and P. Rigny, *Inorg. Nucl. Chem. Suppl.*, 131 (1976).
(29) These molar ratios are relative to the initial amount of materials, and due to a possible precipitation of a solid complex, e.g., MUF_7 or M_2UF_8; the actual composition may deviate from these figures.
(30) R. Bougon, unpublished data. Since this work, we have been aware of the work of J. Berry et al. on the oxidizing and fluoride ion acceptor properties of UF_6 in acetonitrile which is in agreement with our findings.
(31) A. Prescott, D. W. A. Sharp, and J. M. Winfield, *J. Chem. Soc.*, Dalton *Trans.*, 934 (1975).
(32) A. Prescott, D. W. A. Sharp, and J. M. Winfield, *J. Chem. Soc., Dalton Trans.*, 936 (1975).
(33) E. L. Muetterties, *Inorg. Chem.*, **4**, 769 (1965).
(34) A. J. Dianoux and P. Rigny, *J. Phys.*, **29**, 791 (1968).
(35) A. J. Dianoux, Thesis, Lyon, 1969.
(36) J. L. Person, Thesis CNAM, Paris, 1975.
(37) R. A. Penneman, G. D. Sturgeon, L. B. Asprey, and F. H. Kruze, *J. Am. Chem. Soc.*, **87**, 5803 (1965).
(38) J. L. Hoard, *J. Am. Chem. Soc.*, **61**, 1252 (1939).
(39) G. L. Brown and L. A. Walker, *Acta Crystallogr.*, **20**, 220 (1966).
(40) Pr. N. Bartlett, private communication.
(41) S. P. Beaton, Ph.D. Thesis, University of British Columbia, 1966.
(42) E. G. Ippolitov and P. A. Koz'min, *Dokl. Akad. Nauk SSSR*, **5**, 1081 (1962).

Contribution from Bell Laboratories,
Murray Hill, New Jersey 07974

Photoacoustic Spectroscopy of Iridium Carbonyl Halide Linear-Chain Conductors

A. ROSENCWAIG, A. P. GINSBERG,* and J. W. KOEPKE

Received April 12, 1976 AIC60281T

Optical studies of polycrystalline linear-chain conductors are of considerable current interest. However, these materials are generally highly light-scattering and thus difficult to study by conventional optical transmission or reflection techniques. Photoacoustic spectroscopy offers a highly effective means for obtaining optical spectra on such materials, and we report here the first photoacoustic study of this class of materials in the 250–1000-nm range, in particular, of the compounds $K_{0.60}Ir(CO)_2Cl_2 \cdot 0.5H_2O$, $K_{0.98}Ir(CO)_2Cl_{2.42} \cdot 0.2CH_3COCH_3$, $(TTF)_{0.61}Ir(CO)_2Cl_2$ (TTF = tetrathiafulvalenium), and $Cs_{0.60}Ir(CO)_2Br_2$. These compounds contain conducting linear chains of square-planar *cis*-$[Ir(CO)_2X_2]^{0.6-}$ (X = Cl, Br) units. Their photoacoustic spectra show three absorption bands below 650 nm at 2.3, 2.9, and ~3.4 eV, which are assigned as metal-to-ligand charge-transfer transitions from the a(yz) and b(xz) metal orbitals to the predominantly ligand CO b(π^*, $6p_z$) orbital. Above 650 nm the spectrum rises strongly toward the infrared region. This rise is the high-energy end of a broad absorption band extending from ~0.1 to 2 eV as subsequently shown by conventional infrared transmission spectroscopy. It is assigned as the transition from the $5d_{z^2}$ band to b(π^*, $6p_z$). The width and energy of this transition appear to depend upon chain length, exhibiting a significant broadening and shift to higher energy upon crushing of the sample. All of the observed linear-chain transitions are considerably red-shifted with respect to the corresponding transitions in nonchain $[Ir(CO)_2Cl_2]^-$. The red shift is attributed to interactions along the chain which raise the energy of a(yz), b(xz), and a(z^2) and lower the energy of b(π^*, $6p_z$).

Polycrystalline linear-chain conductors are generally highly light-scattering materials that are quite difficult to study in the optical region by conventional transmission or reflection spectroscopy. Since optical spectra of these materials are of considerable interest in providing information about their electronic structure, linear-chain conductors are excellent candidates for examination by the newly developed technique of photoacoustic spectroscopy.[1-3] In this paper we describe a photoacoustic study of the recently characterized compounds[4] $K_{0.60}Ir(CO)_2Cl_2 \cdot 0.5H_2O$, $K_{0.98}Ir(CO)_2Cl_{2.42} \cdot 0.2CH_3COCH_3$, $(TTF)_{0.61}Ir(CO)_2Cl_2$ (TTF = tetrathiafulvalenium), and $Cs_{0.60}Ir(CO)_2Br_2$. These compounds all contain conducting linear chains of square-planar *cis*-$[Ir(CO)_2X_2]^{0.6-}$ (X = Cl, Br) units, as illustrated in Figure 1.

In photoacoustic spectroscopy of solids, light absorbed by a solid sample is detected as an acoustic signal. It has been possible with this technique to obtain optical absorption spectra of almost any type of material, irrespective of whether the sample is crystalline or amorphous, a powder or a gel. Since only the *absorbed* light is converted to sound, scattered light, which presents such a severe problem when dealing with many solid materials by conventional means, presents no major problem in photoacoustic spectroscopy. Our results for the *cis*-$[Ir(CO)_2X_2]^{0.6-}$ linear chains show several notable features. In particular, we find that the linear chains have a near-ir absorption of variable frequency, apparently dependent on the chain length and not present in *cis*-$[Ir(CO)_2Cl_2]^-$ in the absence of chain formation. Also, the uv–visible region absorption of the chain complex is significantly red-shifted in comparison to nonchain $[Ir(CO)_2Cl_2]^-$, contrary to what might be expected in view of the higher Ir oxidation state in the chain complex. These effects are attributed to metal–metal interaction along the chain axis which results in band formation and raises the energy of the d levels from which the observed transitions originate.

Experimental Section

$K_{0.60}Ir(CO)_2Cl_2 \cdot 0.5H_2O$, $K_{0.98}Ir(CO)_2Cl_{2.42} \cdot 0.2CH_3COCH_3$, $(TTF)_{0.61}Ir(CO)_2Cl_2$, and $Cs_{0.60}Ir(CO)_2Br_2$ were prepared and characterized as described previously.[4] $(C_6H_5)_4As[Ir(CO)_2Cl_2]$ was prepared by the method of Forster[5] and characterized by its ir spectrum. Photoacoustic spectra in the range 250–1000 nm were obtained as described elsewhere;[1-3] the polycrystalline powders were studied both before and after grinding in an agate mortar. The absorption spectrum of $K_{0.98}Ir(CO)_2Cl_{2.42}$ in the region 600–17 000 nm was also determined with a Cary Model 14 R spectrophotometer (600–2500 nm) and a Perkin-Elmer Model 457 IR spectrophotometer

Table I. Photoacoustic Spectral Data

$(C_6H_5)_4As[Ir(CO)_2Cl_2]$		$K_{0.98}Ir(CO)_2Cl_{2.42}$		$K_{0.60}Ir(CO)_2Cl_2 \cdot 0.5H_2O$		$(TTF)_{0.61}Ir(CO)_2Cl_2$		$Cs_{0.61}Ir(CO)_2Br_2$	
cm^{-1}	eV	cm^{-1}	eV	cm^{-1}	eV	cm^{-1}	eV	cm^{-1}	eV
		~27300	~3.38	~27300	~3.38	~27300	~3.38	~27300	~3.38
28800	3.57	23200	2.88	23400	2.90	23000	2.85	~23500	~2.91
27000	3.35	18800	2.33	18700	2.32	~19300	~2.39	~19000	~2.4
		7000	0.9–crushed sample						
		5000	0.6–"as made" sample						
		1700	0.21–film						

[a] The high-energy end of this band is seen in the photoacoustic spectra of all of the chain complexes, but the maximum is outside the range of the spectrometer. The approximate maxima listed were determined by conventional transmission spectroscopy.

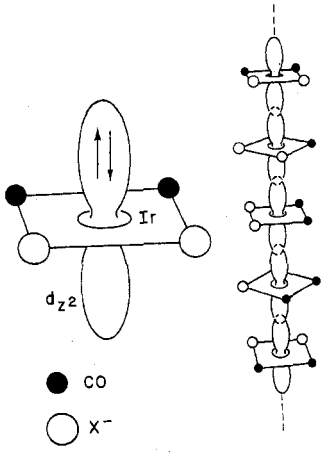

Figure 1. Linear-chain structure of $[Ir(CO)_2X_2]^{0.6-}$ (X = Cl, Br) showing overlap of $5d_{z^2}$ orbitals.

(2000–17000 nm). Samples for these measurements were polycrystalline films prepared by evaporation of acetone solutions on quartz or KCl plates or mineral oil "mulls" prepared both with and without grinding. An equal thickness of substrate material was placed in the reference beam of the spectrophotometer for the optical absorption measurements.

Results

Figure 2 shows the photoacoustic spectra (250–1000 nm) of the linear-chain iridium carbonyl halides and also of the nonchain complex $(C_6H_5)_4As[Ir(CO)_2Cl_2]$; the observed band energies are summarized in Table I. We note that the spectra of all four linear chain complexes have two distinct intense absorption regions. The high-energy visible and uv absorption clearly displays band structure, while the low-energy visible and near-ir region appears as a rather unstructured background that rises toward the infrared region. $K_{0.98}Ir(CO)_2Cl_{2.42}$ and $K_{0.60}Ir(CO)_2Cl_2 \cdot 0.5H_2O$ have essentially identical spectra in the 300–600-nm region: there are two partially resolved bands (2.3 and 2.9 eV) and a poorly defined shoulder (~3.4 eV). $(TTF)_{0.61}Ir(CO)_2Cl_2$ appears to have a similar spectrum in this region, but the band pattern is distorted and increased in intensity by the presence of unresolved underlying TTF absorption.[6] $Cs_{0.61}Ir(CO)_2Br_2$ has a uv–visible absorption pattern similar to the carbonyl chloride linear chains; however, in this sample, the high-energy band (~3.4 eV) is better resolved while the two low-energy bands (~2.9 and 2.4 eV) are partially obscured by the tail of the ir absorption. By contrast, $(C_6H_5)_4As[Ir(CO)_2Cl_2]$ shows no evidence of absorption in the near-ir region while in the 300–600-nm region two bands (3.4 and 3.6 eV) are seen.

Our present photoacoustic spectrometer does not cover the region of the ir band maximum; the entire band was, however, subsequently observed by conventional transmission spectroscopy on samples of $K_{0.98}Ir(CO)_2Cl_{2.42}$ (Figure 3 and Table I). The position and width of this band is sensitive to the method of sample preparation. A film obtained by evaporating

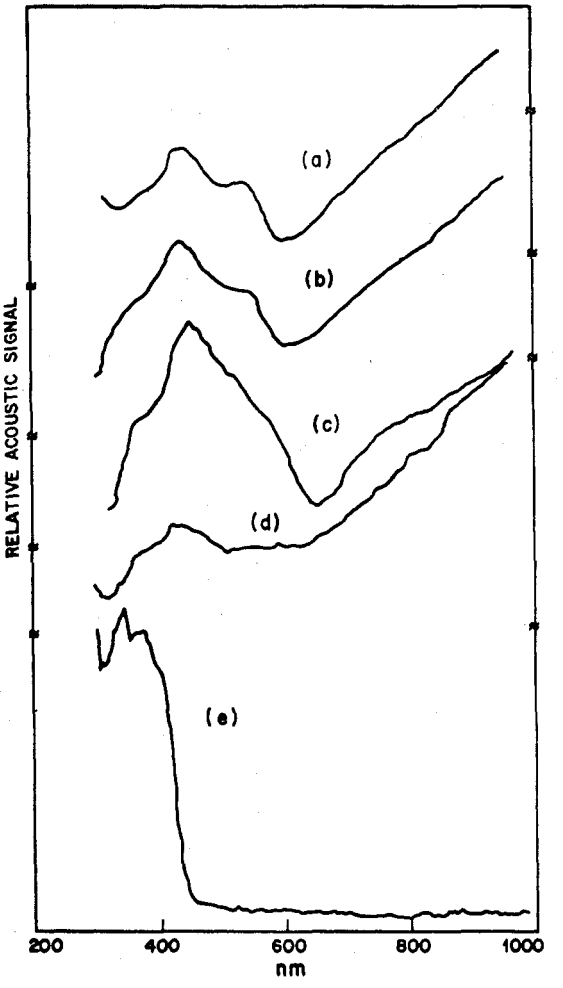

Figure 2. Photoacoustic spectra of "as made" samples of (a) $K_{0.98}Ir(CO)_2Cl_{2.42} \cdot 0.2CH_3COCH_3$, (b) $K_{0.60}Ir(CO)_2Cl_2 \cdot 0.5H_2O$, (c) $(TTF)_{0.61}Ir(CO)_2Cl_2$, (d) $Cs_{0.61}Ir(CO)_2Br_2$, and (e) $(C_6H_5)_4As[Ir(CO)_2Cl_2]$.

an acetone solution of the compound has an ir absorption extending from ~0.1 to ~1.2 eV with a maximum at 0.21 eV. With a mineral oil mull prepared without crushing the "as made" sample, the band is broader and the maximum has shifted to higher energy (0.6 eV). A further shift to higher energy (0.9 eV) and further broadening are observed if the sample is well crushed before preparing the mull. The effect of crushing in broadening the ir band and shifting it to higher energy is also demonstrated by the photoacoustic spectra of crushed samples shown in Figure 4. It is seen that in the crushed samples the tail of the ir band overlaps the uv–visible absorptions much more strongly than in the uncrushed samples.

We are aware that $[Pt(NH_3)_4][PtCl_4]$, which contains linear chains of *weakly* interacting platinum atoms, appears

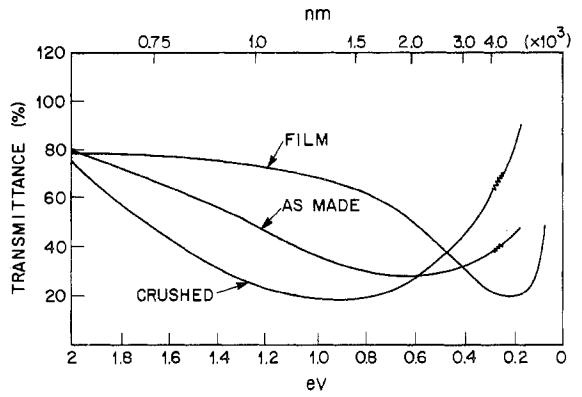

Figure 3. Near-ir absorption of $K_{0.98}Ir(CO)_2Cl_{2.42}$ as determined by conventional transmission spectroscopy.

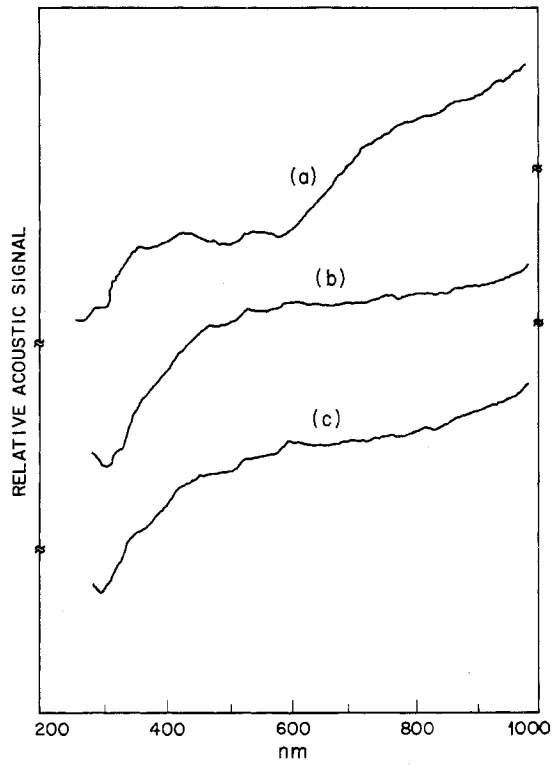

Figure 4. Photoacoustic spectra of crushed samples of (a) $K_{0.98}Ir(CO)_2Cl_{2.42}$, (b) $(TTF)_{0.61}Ir(CO)_2Cl_2$, and (c) $Cs_{0.61}Ir(CO)_2Br_2$.

to have a strong, broad absorption band in the near-ir region centered at ~6000 cm^{-1} (0.7 eV) when studied in a mull or KCl disk and that this band has been shown to be a spurious effect arising from differences in light scattering between the sample and reference.[7] Conventional light scattering cannot however strongly affect a photoacoustic spectrum, particularly in a region where there is no real absorption, since such light scattering is solely equivalent to an increase, by a factor of 2 or 3 at the most, of the sample thickness. Only in the presence of a strong absorption does light scattering have to be taken into account, since then it will result in a somewhat stronger photoacoustic signal. Since our photoacoustic spectra clearly show a strong signal increasing in intensity toward the infrared region, we conclude that the near-ir band must be real and is probably the result of electronic transitions in the linear-chain iridium complexes.

Discussion

$(C_6H_5)_4As[Ir(CO)_2Cl_2]$ contains $5d^8$ Ir(I) in cis square-planar coordination,[5] point group symmetry C_{2v}. In Figure 5 we show two simplified schematic molecular orbital energy

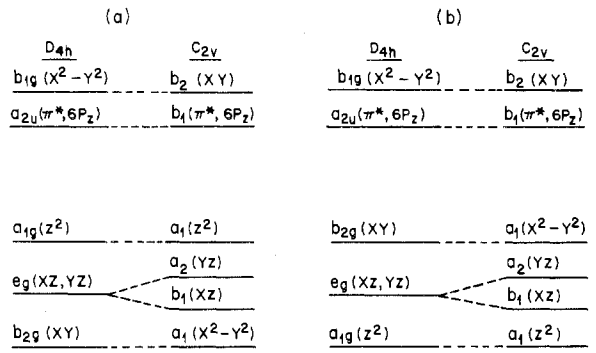

Figure 5. Schematic molecular orbital energy level diagrams for square-planar C_{2v} $[Ir(CO)_2Cl_2]^-$ and their relation to the D_{4h} case: (a) based on the $Pt(CN)_4^{2-}$ MO diagram of ref 8; (b) based on the $Pt(CN)_4^{2-}$ MO diagram determined by an SCF-Xα-SW calculation.[10]

level diagrams in terms of which the optical absorption of $[Ir(CO)_2Cl_2]^-$ may be described. The symmetry assignments refer to a right-handed coordinate system with the x axis along the C_2 axis of C_{2v} and the z axis perpendicular to the molecular plane. Figure 5a shows the level scheme derived from the $Pt(CN)_4^{2-}$ (D_{4h}) MO diagram of Piepho, Schatz, and McCaffery[8] and used to interpret the spectrum of *cis*-$Pt(NH_3)_2(CN)_2$ and related compounds.[9] Figure 5b shows the level ordering expected on the basis of the MO diagram recently determined[10] by an SCF–Xα–SW calculation for $Pt(CN)_4^{2-}$. The two level schemes differ in interchanging the positions of $a_1(z^2)$ and $a_1(x^2 - y^2)$. For Figure 5a the highest occupied level of $[Ir(CO)_2Cl_2]^-$ is $a_1(z^2)$ while for Figure 5b it is $a_1(x^2 - y^2)$. In either case the ground state is $(a_1^2b_1^2a_2^2a_1^2)^1A_1$.

In view of the intense nature of the 3.35- and 3.57-eV bands[11] of $(C_6H_5)_4As[Ir(CO)_2Cl_2]$ and by analogy with the assignments that have been made for the lowest energy intense bands of the $5d^8$ complexes $Pt(CN)_4^{2-}$,[8-10] *cis*-$Pt(NH_3)_2(CN)_2$ and related compounds,[9,12] and ML_2^+ (M = Rh(I), Ir(I); L = di(tertiary phosphine))[13] we assign these bands as the lowest energy-allowed metal-to-ligand charge-transfer (MLCT) transitions from the d or "d-like"[10] levels to the $b_1(\pi^*, 6p_z)$ orbital. The latter orbital is assumed to be mainly an antibonding CO π orbital with some admixed Ir $6p_z$, which also has b_1 symmetry; the $6p_z$ orbital itself lies above $b_2(xy)$. In the absence of spin–orbit coupling the two fully allowed MLCT transitions of lowest energy are $a_1(z^2)$ (or $a_1(x^2 - y^2))^1A_1 \rightarrow b_1(\pi^*, 6p_z)^1B_1$ and $a_2(yz)^1A_1 \rightarrow b_1(\pi^*, 6p_z)^1B_2$. Spin–orbit coupling cannot, however, be neglected for Ir(I) ($\zeta \approx 3000$ cm^{-1}); its effect on the symmetry representations of the excited states arising from one-electron excitations to the configurations $a_1(z^2)$ (or $a_1(x^2 - y^2))b_1(\pi^*, 6p_z)$ and $a_2(yz)b_1(\pi^*, 6p_z)$ is as follows: $(a_1b_1)^1B_1 \rightarrow B_1$; $(a_1b_1)^3B_1 \rightarrow A_2, A_1, B_2$; $(a_2b_1)^1B_2 \rightarrow B_2$; $(a_2b_1)^3B_2 \rightarrow A_2, B_1, A_1$. Transitions from the $^1A_1$ ground state to A_2 excited states are not dipole allowed under C_{2v} symmetry, while transitions to the low-lying $A_1(^3B_1)$ state will be very weak since there is no nearby A_1 state of singlet origin to enhance its intensity. Transitions to $B_2(^3B_1)$ should, however, have enhanced intensity because of admixture with the nearby $B_2(^1B_2)$ state. We therefore suggest the assignment $a_1(z^2)$ (or $a_1(x^2 - y^2))^1A_1 \rightarrow b_1(\pi^*, 6p_z)B_2(^3B_1)$, probably overlapped with $a_2(yz)^1A_1 \rightarrow b_1(\pi^*, 6p_z)B_1(^3B_2)$, for the 3.35-eV band of $[Ir(CO)_2Cl_2]^-$; this is analogous to Isci and Mason's[9] assignment for the lowest energy MLCT band in Pt(en)$(CN)_2$ and *cis*-$Pt(NH_3)_2(CN)_2$. The 3.57-eV band is then assigned as predominantly $a_1(z^2)$ (or $a_1(x^2 - y^2))^1A_1 \rightarrow b_1(\pi^*, 6p_z)B_1(^1B_1)$, analogous to Isci and Mason's[9] assignment for the next to the lowest energy MLCT band of Pt(en)$(CN)_2$ and *cis*-$Pt(NH_3)_2(CN)_2$.

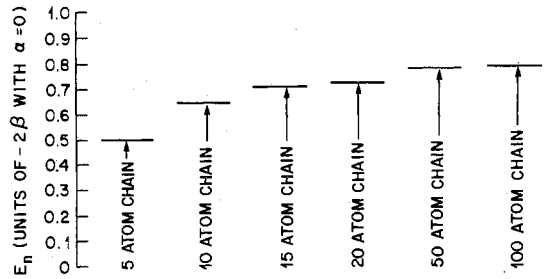

Figure 6. Tight binding band theory energies of the highest filled d_{z^2}-band level of $[Ir(CO)_2Cl_2]^{0,6-}$ as a function of chain length. The energy is given in units of -2β with α taken as zero. The observed near-ir band is assumed to be due to transitions from this d_{z^2} band to a higher unfilled b(π^*, $6p_z$) band.

In $[Ir(CO)_2X_2]^{0.6-}$ linear chains the cis square-planar units are linked by strong metal–metal bonds[14] formed principally by overlap of Ir $5d_{z^2}$ orbitals along the chain axis (Figure 1); the iridium is partially oxidized over Ir(I) to give an effective oxidation state of 1.4. The strong metal–metal interaction presumably drastically raises the energy of the d_{z^2} band of states, as has been suggested for the platinum cyanide chain complexes,[10] and we propose that in $[Ir(CO)_2X_2]^{0.6-}$ chains the d_{z^2} band has been raised to a sufficiently high energy that transitions from it to $b_1(\pi^*, 6p_z)$ give rise to the broad absorption observed between 0.1 and 2 eV. A possible explanation for the shift of this absorption to higher energy when the sample is crushed is illustrated in Figure 6; this shows the tight binding band theory energy of the highest filled level of the d_{z^2} band as a function of chain length. These energies were calculated from the relation[15]

$$E_n = \alpha + 2\beta \cos(n\pi/(N+1))$$

where $\alpha = \int \varphi_i^* H \varphi_i \, d\tau$, $\beta = \int \varphi_i^* H \varphi_{i+1} \, d\tau$ (φ_i is the $5d_{z^2}$ wave function of the ith atom in the chain), N is the number of atoms in the chain, and $n = 1, 2, \ldots, N$; the highest filled level has $n = 0.8N$. It is seen that, for short chains (below about 100 atoms in length), this model predicts a significant decrease in the energy of the highest occupied level with decreasing chain length. If crushing the sample in a mortar and pestle causes extensive chain breakage, as one would expect, then this model predicts a shift in the near-ir band edge to higher energy. This prediction is in qualitative agreement with our results. However the tight binding band theory model is unable to account for the shift to higher energy of the centroid of the ir band and for the increased width of this band upon sample crushing. This is not surprising in light of the approximations present in the model. Moreover, both the centroid shift and the increased line width may be due, in part, to a broader distribution of chain lengths in the crushed samples. That chain length distribution might play a significant role is indicated by the fact that the film which was obtained by evaporation of a solution of the sample and which presumably contained the narrowest distribution and the longest chain lengths gave rise to the narrowest and lowest energy near-ir band.

The above interpretation of the effect of crushing on the near-ir absorption is consistent with the observation[16] that after grinding in a mortar and pestle the resistivity ρ of a sample of $K_{0.98}Ir(CO)_2Cl_{2.42}$ still followed the relation

$$\rho = \rho_0 \exp(T_0/T)^{1/2}$$

with essentially the same value of the parameter T_0 as before grinding ($T_0 = 8.6 \times 10^3$ K before grinding[4] and 1.1×10^4 K after grinding), but its resistivity had increased by a factor of ~ 3. A recent analysis of hopping conductivity in "one-dimensional" compounds indicates that T_0 should be essentially independent of chain length.[17] Chain breakage by sample crushing would therefore not be expected to affect T_0. Chain breakage does, however, decrease the number of low-resistance pathways for conduction and must therefore increase the total resistance.

In terms of the level scheme in Figure 5a, the near-ir band of the linear chains corresponds to the 3.57- and 3.35-eV bands of $[Ir(CO)_2Cl_2]^-$, strongly red-shifted by the metal–metal interaction. The high-energy optical absorptions of the linear chains can now be assigned as MLCT transitions from a(yz) and b(xz) to b(π^*, $6p_z$) (the subscripts on the symmetry designations have been dropped on the assumption that the only overall symmetry element retained by the chain is a $c_2(x)$ axis). By analogy with assignments made for $Pt(en)(CN)_2$ and *cis*-$Pt(NH_3)_2(CN)_2$[9] we suggest $a(yz)^1A \rightarrow b(\pi^*, 6p_z)B(^3B)$ for the 2.3–2.4-eV band, $a(yz)^1A \rightarrow b(\pi^*, 6p_z)B(^1B)$ for the 2.9-eV band, and $b(xz)^1A \rightarrow b(\pi^*, 6p_z)B(^3A_1)$ for the 3.4-eV band. These absorptions are considerably red-shifted with respect to the corresponding transitions in nonchain $[Ir(CO)_2Cl_2]^-$. This is contrary to the expected increase in energy of MLCT transitions with increasing oxidation state of the metal. We attribute the red shift to increased energy of the a(yz) and b(xz) orbitals, caused by antibonding metal–metal interaction,[18] combined with a decrease in the energy of b(π^*, $6p_z$) caused by weak bonding interaction between these orbitals in the chain. It seems likely that a(yz) and b(xz) will be above a($x^2 - y^2$) in the chain complexes even if the level scheme of Figure 5b is appropriate for $[Ir(CO)_2Cl_2]^-$.

We have also considered two alternative assignments to the one made above for the near-ir band. An obvious possibility is to assign the band as an Ir(I)–Ir(II) or Ir(I)–Ir(III) intervalence transition. We believe this to be inappropriate because there is good evidence[4] that the charges (holes) arising from partial oxidation of $Ir(CO)_2Cl_2^-$ units are delocalized over a segment of the iridium chain. The corresponding assignment for a delocalized system is as an intraband transition between levels of the $5d_{z^2}$ band; this allows the dependence on chain length to be interpreted as before. However, the difficulty arises that the next highest energy absorption (2.3 eV) must now be assigned as a transition from the $5d_{z^2}$ band to $b_1(\pi^*, 6p_z)$. The 2.3-eV band would then be expected to show a chain length dependence similar to that of the near-ir band. Since this is not observed, we believe that assignment of the near-ir absorption as an intraband transition is untenable.

Acknowledgment. We thank Dr. J. J. Hauser for the conductivity measurement on crushed $K_{0.98}Ir(CO)_2Cl_{2.42}$.

Registry No. $(C_6H_5)_4As[Ir(CO)_2Cl_2]$, 15152-88-2; $K_{0.98}Ir(CO)_2Cl_{2.42}$, 58002-47-4; $K_{0.60}Ir(CO)_2Cl_2 \cdot 0.5H_2O$, 58002-48-5; $(TTF)_{0.61}Ir(CO)_2Cl_2$, 58002-50-9; $Cs_{0.61}Ir(CO)_2Br_2$, 58002-52-1.

References and Notes

(1) A. Rosencwaig, *Science*, **181**, 657 (1973).
(2) A. Rosencwaig, *Anal. Chem.*, **47**, 592A (1975).
(3) A. Rosencwaig, *Phys. Today*, **28** (9), 23 (1975).
(4) A. P. Ginsberg, J. W. Koepke, J. J. Hauser, K. W. West, F. J. DiSalvo, C. R. Sprinkle, and R. L. Cohen, *Inorg. Chem.*, **15**, 514 (1976).
(5) D. Forster, *Inorg. Nucl. Chem. Lett.*, **5**, 433 (1969).
(6) A Cary 14R spectrum (300–800 nm) of a mineral oil mull of TTF has absorptions at 305, 319, 371, and 460 nm.
(7) E. Fishman and L. V. Interrante, *Inorg. Chem.*, **11**, 1722 (1972).
(8) S. B. Piepho, P. N. Schatz, and J. A. McCaffery, *J. Am. Chem. Soc.*, **91**, 5994 (1969).
(9) H. Isci and W. R. Mason, *Inorg. Chem.*, **14**, 905 (1975).
(10) L. V. Interrante and R. P. Messmer, *Chem. Phys. Lett.*, **26**, 225 (1974).
(11) Although we cannot give a quantitative measure of band intensity from the photoacoustic spectra, it is clear, by comparison of the photoacoustic signal strength with the signals from known charge-transfer and crystal field transitions in a variety of materials, that these bands are of the order expected for charge-transfer transitions.
(12) H. Isci and W. R. Mason, *Inorg. Chem.*, **14**, 913 (1975).
(13) G. L. Geoffroy, M. S. Wrighton, G. S. Hammond, and H. B. Gray, *J. Am. Chem. Soc.*, **96**, 3105 (1974).

(14) The Ir–Ir distance in several of these compounds has been reported to be 2.86 Å: K. Krogmann and H. P. Geserich, *ACS Symp. Ser.*, No. 5, 350–355 (1974).
(15) J. R. Miller, *J. Chem. Soc.*, 713 (1965).
(16) J. J. Hauser, personal communication.
(17) V. K. S. Shante, C. M. Varma, and A. N. Bloch, *Phys. Rev. B*, **8**, 4885 (1973).
(18) L. V. Interrante and R. P. Messmer, *Inorg. Chem.*, **10**, 1174 (1971).

Contribution from the Departments of Chemistry, University of Notre Dame, Notre Dame, Indiana 46556, and Indiana University, Bloomington, Indiana 47401

Effect of Alkyl Substituents on the First Ionization Potential and on $5d^{10}$ Ionization in Dialkylmercury Compounds

T. P. FEHLNER,*[1a] J. ULMAN,[1a] W. A. NUGENT,[1b] and J. K. KOCHI*[1b]

Received January 22, 1976 AIC60064S

The He I photoelectron spectra of a series of dialkylmercury compounds, symmetrical (R_2Hg) as well as unsymmetrical (RHgR′), have been obtained. These compounds differ significantly from homologous series previously studied by PES in that ionization proceeds from a bonding orbital as opposed to a nonbonding orbital. Consequently, alkyl substituent effects on the first ionization potential along the series of RHgR′ (R′ = methyl, ethyl, isopropyl, *tert*-butyl) exhibit a marked "saturation" effect, in contrast to the "additive" relationship observed in the other species. The origin of this effect is discussed. In contrast, ionization of the 5d electrons, which are not involved in bonding, shows the usual additive dependence on alkyl substitution. Mercury atom charges and electronegativities of the alkyl groups are estimated, based on the shift in the 5d band in R_2Hg from Hg. The sensitivity of the ionization potential to substituent effects in the series of dialkylmercury compounds is found to decrease in the order RHgMe > RHgEt > RHg-*i*-Pr > RHg-*t*-Bu.

Introduction

The uv photoelectron spectra (PES) of some divalent compounds of the group 2B metals, including the ionization from an inner-shell d orbital, have been reported recently.[2-5] Only one of these papers[2a] deals with alkyl derivatives of mercury, and then only briefly. We have examined the PES of an extensive series of mercury dialkyls by systematically varying the structure of the alkyl group from methyl through *tert*-butyl and neopentyl, in order to probe the effect of alkyl substituents. The series of dialkylmercury compounds differs from that of other alkyl-substituted compounds examined previously, in that no high-lying nonbonding electrons are present and the first ionization potential must result from removal of electrons from bonding orbitals. The study of dialkylmercury compounds also allows a direct comparison to be made of alkyl substituent effects on the highest occupied bonding orbital (HOMO), with substituent effects on the ionization from an orbital not directly involved in bonding, viz., the mercury 5d orbitals.

Experimental Section

The photoelectron spectrometer used in these studies has been previously described.[6] The dialkylmercury compounds were prepared in pure form by the general method of Singh and Reddy,[7] and they all gave appropriate NMR, mass spectral, gas chromatographic, and elemental analyses. All of the compounds were sufficiently volatile at room temperature to be admitted directly into the ionization chamber in the gas phase. A xenon–argon mixture was used as an internal calibration standard for each spectrum.

Results and Discussion

The He I photoelectron spectra of dialkylmercury compounds show two principal bands of interest to us. The first ionization potential, occurring in a range between 7.57 eV (di-*tert*-butylmercury) and 9.33 eV (dimethylmercury) is included in a fairly broad, unsymmetrical band. A second, weaker band occurs between 14.4 and 15.0 eV and has been attributed to ionization from the mercury $5d^{10}$ shell.[2a] The ionization energies for these two bands are tabulated in Table I. Representative spectra are reproduced in Figure 1 for one series of alkyl(methyl)mercury compounds, i.e., R–Hg–CH_3. The internal consistency of the data is illustrated in Figure 2 by a comparison of the ionization potentials of the methylmercury alkyls with those of the ethylmercury analogues.

Table I. The First and $5d^{10}$ Vertical Ionization Potentials (eV) of Dialkylmercury Compounds

Compd	1st IP	$5d^{10}$ IP	Compd	1st IP	$5d^{10}$ IP
$(CH_3)_2Hg$	9.33	14.93	$(i\text{-}C_3H_7)_2Hg$	8.03	14.46
$(CH_3)(C_2H_5)Hg$	8.84	14.85	$(C_2H_5)(t\text{-}C_4H_9)Hg$	8.06	*a*
$(C_2H_5)_2Hg$	8.45	14.71	$(i\text{-}C_3H_7)(t\text{-}C_4H_9)Hg$	7.73	*a*
$(CH_3)(i\text{-}C_3H_7)Hg$	8.48	14.86	$(n\text{-}C_4H_9)_2Hg$	8.35	*a*
$(CH_3)(i\text{-}C_4H_9)Hg$	8.75	14.74	$(i\text{-}C_4H_9)_2Hg$	8.30	14.47
$(CH_3)(t\text{-}C_4H_9)Hg$	8.31	*a*	$(t\text{-}C_4H_9)_2Hg$	7.57	*a*
$(C_2H_5)(i\text{-}C_3H_7)Hg$	8.18	14.61	$(i\text{-}C_4H_9)(neo\text{-}C_5H_{11})Hg$	8.33	14.49
$(n\text{-}C_3H_7)_2Hg$	8.29	14.63	$(neo\text{-}C_5H_{11})_2Hg$	8.30	14.41

[a] The intensity of this band was too low to observe it above the noise level of the spectrum.

The effect of alkyl substitution on the first ionization potential of a series of alkyl derivatives is attributed primarily to polarization effects in the molecular ion final state.[8,9] It has been recognized that such electronic effects are additive along the series Me, Et, *i*-Pr, and *t*-Bu.[10] Thus the energy effect of replacing Me by Et is expected to equal that of replacing Et by *i*-Pr or of replacing *i*-Pr by *t*-Bu. In each case, α hydrogens in CH_3 are being sequentially replaced by methyl groups. Such a relationship is observed in chemical equilibria and reaction rates,[10] as well as in ionization potentials determined by PES.[11,12]

A recent relevant example of this additivity relationship involves the proton affinities (PA) of alcohols which were found to increase by increments of 6 ± 1 eV along this series.[13] The equal increments in proton affinities, Δ(PA), are particularly noteworthy, since Martin and Shirley have shown[9] that the variation in proton affinities of this series of alcohols should be equal to the variation in the O(1s) binding energy of the same compounds. Indeed a plot of the proton affinities of alcohols against their ionization potentials is linear with a unit slope. This correlation suggests that both effects arise from the polarization of the alkyl group in response to a unit positive charge on oxygen.

Such additive energy effects have been used by Taft[10] as a criterion for identifying polar effects as denoted by the empirical substituent constant σ^* (Me:Et:*i*-Pr:*t*-Br =